Showcasing research from Dr. Francesco Brandi of Institute of Chemistry of OrganoMetallic Compounds CNR-ICCOM (Italy) and Professor Bert F. Sels. the Center for Sustainable Catalysis and Engineering, KU Leuven (Belgium) *et al.*

The role of Beta zeolites in the selective single *O*-demethylation of alkyl-syringols to alkyl-methoxycatechols, a novel polymer building block class

This study explores the production of methoxycatechols from renewable lignin-derived syringols *via* selective single *O*-demethylation (ODM) using Beta zeolites in hot pressurized water. The usage of Beta zeolite enhances the selectivity for reaction of 4-methylsyringol to 4-methyl-6-methoxycatechol (MMC). Moreover, MMC is applied for the first time as a renewable building block in the synthesis of an epoxy thermoset.

Image reproduced by permission of Francesco Brandi and Bert F. Sels from *Green Chem.*, 2025, **27**, 4512.

Artwork created by Joris Snaet.

As featured in:

See Francesco Brandi, Bert F. Sels *et al.*, *Green Chem.*, 2025, **27**, 4512.

ROYAL SOCIETY OF CHEMISTRY

rsc.li/greenchem

Registered charity number: 207890

Green Chemistry

PAPER

View Article Online
View Journal | View Issue

Check for updates

Cite this: *Green Chem.*, 2025, **27**, 4512

The role of Beta zeolites in the selective single *O*-demethylation of alkyl-syringols to alkyl-methoxycatechols, a novel polymer building block class†

Francesco Brandi, *‡[a,b] Alaa Al-Naji,‡[a] Xian Wu, ‡[a] Rashmi Singh, [a] Laura Trullemans, [a] Ibrahim Khalil, [a] Minrui Xu, [c] Philippe Marion,[c] Sergio Mastroianni[c] and Bert F. Sels *[a]

Received 26th September 2024,
Accepted 20th February 2025

DOI: 10.1039/d4gc04824e

rsc.li/greenchem

Syringyl moieties, the primary phenols in hardwood, represent a valuable resource for bio-based product development. Despite their potential, they are currently treated mostly as waste due to the lack of effective catalytic de/functionalization methods. A promising approach involves the single *O*-demethylation (ODM) of syringyl derivatives, yielding methoxy-catechol moieties (MC)—vicinal hydroxyphenols with a methoxy group—that offer broad yet underexplored applications. This study achieved selective ODM of 4-methylsyringol to 3-methoxy-5-methyl benzene-1,2-diol, or 4-methyl-6-methoxy catechol (MMC) using commercially available acidic Beta zeolites, and hot pressurized water as a green solvent system. Unlike other solid acid or homogeneous catalysts, Beta zeolites exhibited high MMC selectivity (>80 mol%) facilitated by their unique 3D 12-membered ring pore structure, allowing precise stepwise ODM of 4-methyl syringol (MSyr). Additionally, this study reports, for the first time, the application of MMC epoxy-thermosets *via* glycidylation. The resulting high-performance resin exhibited a glass transition temperature (T_g) of 126 °C, and excellent thermal resistance, with a 5% weight loss temperature ($T_{d5\%}$) of 293 °C in air. This work introduces MMC as a renewable replacement to fossil-derived phenols as a novel polymer building block.

Open Access Article. Published on 25 February 2025. Downloaded on 2/8/2026 3:04:21 PM.
This article is licensed under a Creative Commons Attribution 3.0 Unported Licence.

Green foundation

1. This study explores the production of methoxycatechols from renewable lignin-derived syringols *via* selective single *O*-demethylation (ODM). Traditional *O*-demethylation methods can be enhanced using the microporous solid acid Beta zeolite, as reported in this work. The obtained product 4-methyl-6-methoxycatechol (MMC) is applied for the first time as a potentially new class of renewable building block in the synthesis of an epoxy thermoset.
2. The usage of microporous Beta zeolite in water enhances the selectivity for the single ODM of 4-methylsyringol to MMC. This process employs safe and green catalysts and solvent, aligning with the principles of green chemistry. Moreover, MMC is a promising bio-based alternative to fossil-derived building blocks.
3. Future studies are necessary to expand the application field of MC moieties as building blocks for new bio-based polymers, fragrances, and antioxidants.

Introduction

To mitigate society's environmental footprints and promote sustainability, it is crucial to explore alternative renewable feedstocks of fossil-derived carbon.[1–3] Lignin is a phenolic biopolymer comprising approximately 25 wt% of lignocellulosic biomass, currently treated as a waste, and emerges as the most abundant renewable source of aromatics on the planet.[4–6] Emerging biorefinery technologies named lignin-first

[a]*Center for Sustainable Catalysis and Engineering, KU Leuven, Celestijnenlaan 200F, 3001 Leuven, Belgium. E-mail: francesco.brandi@cnr.it, bert.sels@kuleuven.be*
[b]*Consiglio Nazionale delle Ricerche, Istituto di Chimica dei Composti Organo Metallici, Via Madonna del Piano 10, 50019 Sesto Fiorentino, Firenze, Italy*
[c]*Syensqo, Research and Innovation Center of Lyon, 85 Avenue des Frères Perret, 69192 Saint Fons, France*

†Electronic supplementary information (ESI) available. See DOI: https://doi.org/10.1039/d4gc04824e

‡These authors equally contributed to the manuscript.

This journal is © The Royal Society of Chemistry 2025

Open Access Article. Published on 25 February 2025. Downloaded on 2/8/2026 3:04:21 PM. This article is licensed under a Creative Commons Attribution 3.0 Unported Licence.

approaches, and especially the reductive catalytic fraction (RCF) strategy have recently demonstrated the potential to produce phenolic monomers from woody biomass's lignin in high yields.[7–12] In addition, thermal methodologies such as fast- or catalytic-pyrolysis produce a condensed oil rich in lignin-aromatics as a by-product of char and bio-gas production.[13]

Those monomers compositions closely resemble the structure of the used native lignin, typically characterized as alkylated phenols. These phenols may lack, or contain one, or two *ortho*-methoxy groups, and are referred to as *p*-hydroxyphenyl-(H) guaiacyl-(G) and synapyl-(S) units, respectively.[13,14] Nevertheless, for lignin-derived monomers to be incorporated into the value chain, specific purification and/or chemical modification, are required through downstream processing subsequent to the lignin-first biorefinery process.[14,15] These chemical modifications, such as functionalization or defunctionalization strategies are tailored to meet specific applications. Particularly, selective cleavage strategies of C–O bonds without breaking other bond are gaining importance for lignin valorization.[16] Among these strategies, *O*-demethylation (ODM) is emerging as an effective strategy to convert the *ortho*-methoxy group into a more reactive phenolic OH.[17,18]

ODM can be considered as a hydrolysis reaction, and involves the cleavage of the *ortho*-aryl-methyl ether bond under the action of water, to form the phenol using stoichiometric (nucleophilic reactant) or catalytic (involving both Brønsted and Lewis) reactions.[17] ODM has been employed in synthetic organic chemistry as a deprotection methodology and has also been applied to produce vicinal phenols from lignin, such as catechol and gallol species.[17,19–21] Moreover, ODM performed in hot pressurized water has been proved to be an efficient and green method to cleave methyl aryl ethers.[16,19]

Currently, the lignin-ODM has principally targeted guaiacyl units to yield catechols, employing both homogeneous and heterogeneous acid catalysts. Common homogeneous acids employed are protic acids, such as HCl,[18] H_2SO_4,[21,22] and HBr,[23] as well as Lewis acids, like LiBr,[24] BBr_3,[25] and TMSI.[26] Despite the fact that homogeneous catalysts achieve high efficiency in guaiacyl unit ODM, the usage of heterogeneous catalysts is preferred for reusability, safety, and the absence of corrosion issues.[16] However, heterogeneous catalysts, including metal oxides like ZrO_2,[19] TiO_2,[19,27] Nb_2O_5,[19,20] and zeolites[19,21] are less prevalent. Notably, 12-member ring zeolites, such as Beta zeolites, have recently demonstrated promising efficiency in guaiacol ODM in hot water.[19,22] Moreover, Beta zeolites have exhibited a higher turnover frequency (TOF, per proton) than homogeneous mineral acids (*e.g.*, HCl) for hydrolysis of methyl, ethyl-, and propylguaiacol in water at 205 °C.[23] This study distinctively highlighted the enhanced activity of ODM in confined spaces, as opposed to traditional homogeneous acids.

While most research has focused on guaiacyl units, syringyl units also warrant attention. Syringyl units are key components of hardwoods, often found as sawdust waste generated during lumber cutting processes.[24] Notably, unlike guaiacyl moieties, containing a single methoxy group, syringyl units possess two chemically equivalent methoxy groups, allowing for two ODM reactions. The first ODM step produces a methoxy catechol (MC) moiety, followed by a second ODM step that yields a gallol (Gal) moiety, as depicted in Scheme 1. However, few examples of syringyl (Syr) valorisation through ODM have been reported in the literature. Similar to guaiacyl ODM, syringyl ODM typically relies on homogeneous acids, primarily HCl and H_2SO_4, at temperatures ranging from 110 °C to 250 °C (refer to Table S2 in the ESI†).[19,25–29] Additionally, few studies have explored the usage of heterogeneous catalysts for Syr ODM. The Maes group patented Beta zeolites for propyl-Syr ODM in water at 275 °C, 75 bar N_2, for 3 h, obtaining 51% of propyl-Gal and 16% of propyl-MC.[30] Abu-Omar *et al.* obtained propyl-Gal (96% yield) and the MC moiety (4% 4-propyl-2-methoxy catechol) from propyl-Syr using Nb_2O_5 at 230 °C in H_2O with 10 bar of extra N_2 pressure during 20 h.[21] These examples focused on complete two-fold Syr ODM to produce Gal moieties, considering MC as a by-product, *viz*. Scheme 1.

Although gallol (Gal) moieties have existing applications, the single ODM product, methoxy catechol (MC), also holds promise, though its potential uses have yet to be demonstrated.

Additionally, Gal moieties are unstable under hydrothermal conditions, where they are prone to condensation and char formation, posing a challenge for their practical utilization.[17,25,31,32] Chemically, MC provides two vicinal phenolic hydroxyl groups, similar to catechol, making it suitable for a variety of functionalization reactions, including esterification, arylation, urethanisation, and silylation. This versatility opens up a wide range of potential applications such as for building block for polymers, pharmaceuticals, agrochemicals, fragrances, and as an antioxidant.[17,33] Additionally, the two vicinal hydroxyl groups make MC a potential building block for active pharmaceutical ingredients and may also impart valuable antioxidant properties.[34] Furthermore, MC contains an *ortho*-methoxy group, akin to guaiacol, which has been demonstrated to enhance the mechanical performance of the resulting polymers.[35–37] Additionally, *ortho*-methoxy-substituted phenols show a marked reduction in *in vitro* estrogenic activity, that leads MC being a potentially more safe chemical

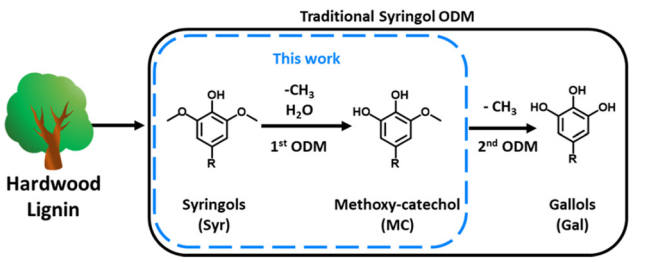

Scheme 1 General reaction scheme of a traditional *O*-demethylation (ODM) of hardwood-lignin derived syringol (Syr) toward methoxy catechol (MC) and gallols (Gal) in the presence of water. This work focuses on the single ODM in water, highlighted in blue, with R = H, Me, and Prop.

Open Access Article. Published on 25 February 2025. Downloaded on 2/8/2026 3:04:21 PM.
This article is licensed under a Creative Commons Attribution 3.0 Unported Licence.

by design than Gal.[38,39] Moreover, in the case of single ODM, only one methyl is removed from the reactant, intrinsically resulting in less by-product formation and a higher atom economy (AE) than what results from the two-fold ODM.

Despite their potential, MC moieties have been studied very little, and no applications have been demonstrated to date. Notably, MC moieties emerge as by-products during the pyrolysis of S-lignin.[40] One promising application of MC moieties is in the synthesis of epoxy thermosets. Particularly, MC may be used as bio-based diphenols to substitute oil-derived ones, among the others bisphenols. To this end, MC moieties are a potentially new, yet undiscovered class of building block, completely different from Gal moieties.

In this regard, Abu-Omar *et al.* successfully synthesized an epoxy thermoset by curing a mixture of propyl-Syr and propyl-MC, using only a 4 mol% concentration of MC.[41] However, the role of MC in thermosets remains unclear due to its low concentration. Additionally, the production of epoxy thermosets necessitates functionalization through a glycidylation step (Scheme 2). Despite this method is well-established, the glycidylation of vicinal phenols (catechols) is often associated with the formation of unwanted benzodioxane moieties.[42] Although the presence of benzodioxanes is known to lower the epoxy resin's onset curing temperature by catalysing the amine-epoxy curing reaction, the impact of these benzoxazines on the final thermal and mechanical properties of the resin remains unclear.[43] While the presence of benzodioxanes is known to reduce the onset curing temperature of epoxy resins by catalysing the amine-epoxy curing reaction, their impact on the final thermal and mechanical properties of the resin remains unclear.

Furthermore, the formation and role of these moieties in the curing process and their effects on polymer properties are not yet understood.

In this study, we advance the applicability of renewable phenols by reporting the selective one-pot ODM of renewable lignin-derived 4-methyl-syringol (MSyr) to produce 5-methyl-3-methoxy catechol (MMC) using acidic Beta zeolite as a catalyst and hot pressurized water as a green solvent. Noteworthy, methyl-substituted syringols is a products of from both lignin-first approach and pyrolysis processes, and for this reason has been selected.

The resulting MMC moiety is then utilized as a precursor for epoxy thermosets to demonstrate its applicability. To achieve this, glycidylation with epichlorohydrin (EC) is employed as a functionalization strategy, followed by curing with isophorone diamine (IPDA). It is noteworthy that the reaction between MMC, or any MC moiety, and epichlorohydrin (EC) has not been previously reported. Therefore, MMC is used in this work as a model compound for the entire MC family.

Overall, this study outlines a comprehensive valorisation strategy that effectively transforms waste-derived syringol from hardwood into an innovative end product, as illustrated in Scheme 2. By repurposing this by-product, the research not only tackles the challenge of waste management but also demonstrates the potential for generating valuable materials from what would otherwise be considered a waste stream. This approach underscores the importance of sustainability in resource utilization and highlights a promising pathway for maximizing the value of hardwood resources.

Results and discussion

Catalytic ODM of MSyr

In this study, 4-methyl-syringol (MSyr) has been chosen as a model compound that resembles both RCF and pyrolysis products derived from hardwood. MSyr can undergo a two-step *O*-demethylation (ODM) process, yielding 4-methyl 6-methoxy catechol (MMC) and 4-methyl gallol (MGal), as illustrated in Scheme 3. Initially, a range of heterogeneous and homogeneous solid acids were investigated, including Nb_2O_5, various zeolite materials such as ZSM-5 (with Si/Al ratios of 40 and 100), Beta (Si/Al ratio of 75), and HCl, as shown in Fig. 1. The textural properties of these catalysts were characterized

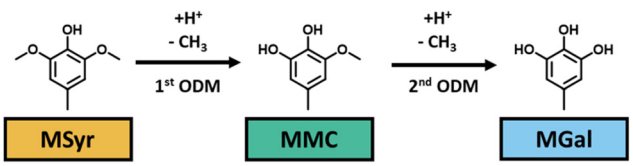

Scheme 3 4-Methyl-syringol (MSyr) twofold ODM to 4-methyl-methoxy catechol (MMC) and to 4-methyl-gallol (MGal).

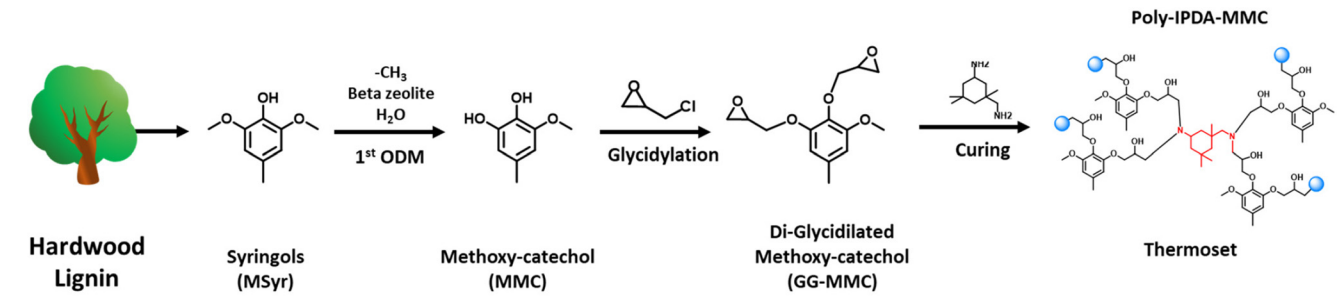

Scheme 2 Proposed valorisation of hardwood lignin-derived syringols involves oxidative demethylation (ODM) followed by glycidylation and curing to produce a partially bio-based epoxy thermoset.

 This journal is © The Royal Society of Chemistry 2025

Open Access Article. Published on 25 February 2025. Downloaded on 2/8/2026 3:04:21 PM.
This article is licensed under a Creative Commons Attribution 3.0 Unported Licence.

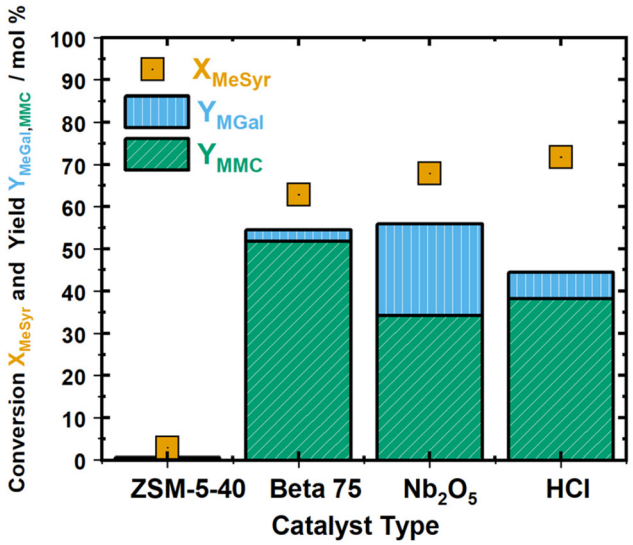

Fig. 1 Conversion of MSyr (X_{MSyr}) and yield of MMC and M-Gal yield (Y_{MMC} and Y_{MGal}) as a function of different used acid catalysts. Reaction conditions for heterogeneous catalysts: temperature: 210 °C, time: 4 h, N_2 pressure = 1 bar, catalyst amount: 200 mg. Reaction conditions for HCl: temperature: 250 °C, time: 1 hour, N_2 pressure = 46 bar- to ensure HCl in liquid state, catalyst amount: 1.45 mmol HCl.

using N_2 physisorption, pyridine FTIR, and XRD, with results reported in Fig. S3 and Table S3 in the ESI.† The selection of different types of zeolites was based on previous studies in the literature, which indicated that Beta 75 exhibited the best performance regarding ODM activity on guaiacol.[20,23] Nb_2O_5 and HCl were selected due to their good performance reported in the literature for guaiacol and propyl-syringol ODM respectively as heterogeneous and homogeneous acids.[20,21] As expected, Beta 75 showed the highest MSyr conversion (X_{MSyr} of 63 mol%) and MMC yield (Y_{MMC} of 52 mol%) among the other tested zeolites, Fig. 1. The low activity for ZSM-5 (X_{MSyr} and Y_{MMC}, respectively 4.7 and 0.6 mol%) is attributed to its smaller 10-membered ring channels (~5.4 Å) compared to the size of studied molecules (>6.5 Å). By changing ZSM-5 from a Si/Al of 40 to 100 (Fig. S3 in ESI†) was not found to increase its activity. In contrast, a lower conversion of MSyr was noticed (Fig. S4 in ESI†).

Interestingly, only a little MGal was formed when using Beta 75 (Y_{MGal} of 2.8 mol%). This is an indication that the reaction in Beta zeolites is suppressing Gal formation in favour of MC moieties. We hypothesize that the micropores of Beta zeolite act as confined reacting spaces enhancing the selectivity towards single ODM products. In such molecular-sized reacting spaces within negative-charged framework of Beta zeolites, the active sites (hydronium ions) are highly organised and localized, hence less mobility. Besides, the strong interaction of hydronium ion cluster with the first methoxy group limits its accessibility with the second methoxy group, resulting in high selectivity to MMC. To compare the activity of Beta 75 with other benchmark heterogeneous catalysts, layered Nb_2O_5 was synthesized following a previously reported procedure.[20,44] Interestingly, Nb_2O_5 showed a similar X_{MSyr} compared to Beta 75 (68 and 62 mol%, respectively), but with different product distributions, particularly with a lower selectivity towards MMC, Fig. 1. When Nb_2O_5 is used, the second ODM step toward Gallol occurs already at lower conversion when compared to Beta 75, which can be attributed to the absence of molecular-sized confinements to the highly exposed acid sites of Nb_2O_5.

For further comparison, the activity of HCl as a homogeneous acid was assessed, resulting in an X_{MSyr} of 72 mol% and Y_{MMC} and Y_{MGal} of 38 mol% and 6.2 mol%, respectively. Notably, black polymeric species were observed in the reaction vessel, suggesting product condensation and explaining the significant gap in the mass balance. It is known that gallol moieties are unstable under hydrothermal conditions and tend to condense.[17] Overall, Beta 75 demonstrated substantially higher selectivity for MMC compared to both Nb_2O_5 and HCl, with selectivity values of 82%, 50%, and 53%, respectively. Additionally, Beta 75 exhibited a lower gap in the mass balance, likely due to the reduced condensation of gallol moieties.

To examine the impact of acid density in zeolites on reaction selectivity, Beta zeolites with varying Si/Al ratios, ranging from 12.5 to 150, were tested. Since the Si/Al ratio does not necessarily correlate linearly with the number of active acid sites (including framework Al, extra-framework Al, and Al aggregates),[45] the density of Brønsted acid sites (BAS) was estimated using pyridine adsorption followed by FTIR spectroscopy (Table S3†). Moreover, it is important to note that the selected Beta zeolites possess similar properties in terms of both specific surface area (515–592 $m^2\ g^{-1}$) and pore volume (0.37–0.46 $cm^3\ g^{-1}$ with exception of Beta 12.5 with 0.90 $cm^3\ g^{-1}$).

The conversion of MSyr was the primary parameter affected by variations in BAS density, exhibiting a peak at a maximum of 183 μmol g^{-1} BAS (X_{MSyr} of 60 mol% and X_{MMC} of 45 mol%), corresponding to the Beta 15 catalyst, as shown in Fig. 2. This is consistent with the ODM of guaiacols in our previous report, where acid density also affected the ODM rates.[23] This finding highlights the importance of host–guest interactions between the zeolites and the reagent in facilitating high reaction rates. In contrast, MMC selectivity remained nearly constant (around 80 mol% all over the screened BAS), suggesting that the BAS is directly involved in enhancing the conversion rate, but only for the first ODM step. The second ODM product, MGal, was detected in significant quantities only at higher BAS densities (180 μmol g^{-1} and above). The consistent value of S_{MMC}, regardless of BAS density, provides compelling evidence for the specific role of Beta zeolite topology in the first ODM step.

Additionally, the reaction profile were monitored at 210 °C over different reaction times, as illustrated in Fig. 3. Consistent with the previous experiments, the selectivity fluctuated around an average value of 80 mol% (79.6 ± 4.8 mol%), while the mass balance remained consistently above 90 mol% (93.3 ± 3.1 mol%), with a slight decrease over time, as shown in Fig. S5.† Moreover, MGal formation was first observed at

Open Access Article. Published on 25 February 2025. Downloaded on 2/8/2026 3:04:21 PM.
This article is licensed under a Creative Commons Attribution 3.0 Unported Licence.

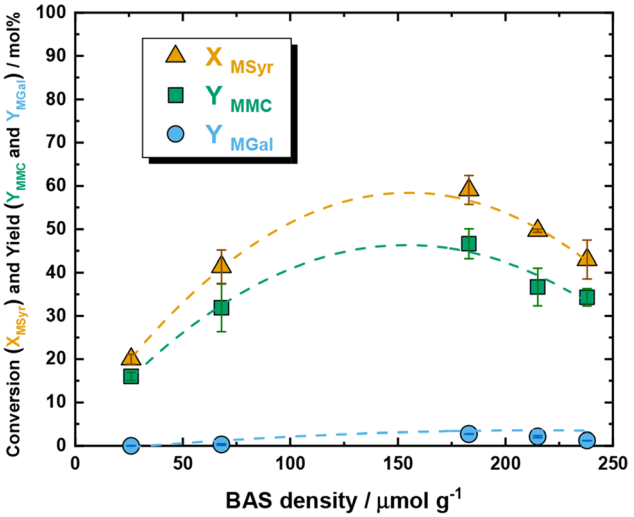

Fig. 2 Conversion of **MSyr** and yield of **MMC** and **MGal** over Beta zeolites as a function of BAS density. Reaction conditions: temperature: 210 °C, time: 2 h, N_2 pressure = 1 bar, catalyst amount: 200 mg. BAS density: 26; 68; 183; 215; 238 µmol g^{-1}.

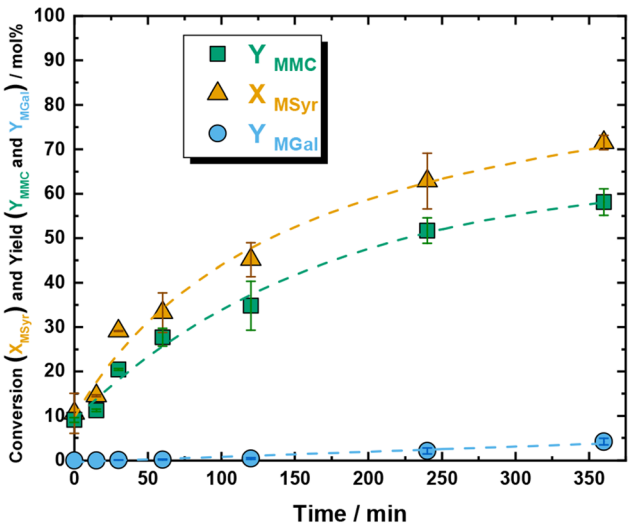

Fig. 3 Conversion of **MSyr** and yield of **MMC** and **MGal** over Beta 75 as a function of time. Reaction conditions: time: 0 min, 15 min, 30 min, 60 min, 120 min, 240 min, 360 min, N_2 pressure 1 bar, catalyst amount: 200 mg, temperature: 210 °C.

120 minutes (S_{MGal} of 0.6 mol%), displaying a linear increase that reached 5.9 mol% after 360 minutes. Similar behaviour was noted in the reaction profiles of Beta 15 and Beta 19, as detailed in Fig. S6 and S7 in the ESI.† When compared, these Beta zeolites exhibited comparable reaction profiles (Fig. S8 in ESI†), with a steady S_{MMC} and a gradual increase in S_{MGal} as reaction time progressed and conversion increased. Notably, the formation of MGal was not associated with a decrease in S_{MMC}, indicating that the two ODM products reached an equilibrium. Based on these reaction profiles, the turnover frequency (TOF) was estimated to be 8.8 h^{-1}, 7.6 h^{-1}, and 22 h^{-1} for Beta 15, 19, and 75, respectively, as shown in Fig. S9 in the ESI.† As reported for methyl guaiacol (MGua), Beta 75 exhibited the highest TOF among the tested Beta zeolites.[22] The TOF of 22 h^{-1} for MSyr is slightly lower than the 24 h^{-1} observed earlier for MGua.[23]

Due to its higher TOF (22 h^{-1}) compared to other Beta zeolites, along with low MGal selectivity (<3 mol%), Beta 75 was chosen for further catalytic investigations. The effect of temperature on MSyr conversion (X_{Msyr}) and product distribution was studied over a range of 190 °C to 250 °C, as shown in Fig. 4. As expected, the rate of X_{Msyr} increased with temperature, rising from a relatively low value of 20 mol% at 190 °C to 91 mol% at 250 °C. Notably, complete conversion was not achieved under the examined conditions.

Furthermore, the MMC selectivity (S_{MMC}) was surprisingly low at 190 °C, accompanied by a significant mass balance gap. However, S_{MMC} remained relatively stable when the temperature increased from the reference point of 210 °C to 230 °C (S_{MMC} values of 77 and 79 mol%, respectively), despite changes in conversion (X_{Msyr} of 45 and 83 mol%, respectively).

Additionally, the second ODM became more pronounced at higher temperatures, with MGal selectivity at 210 °C being low (S_{MGal} of 1.7 mol%) but increasing to 12 mol% and 30 mol% at 230 °C and 250 °C, respectively. Interestingly, the overall mass balance was also found to correlate directly with temperature, peaking at 95 mol% at 250 °C. This mass balance behaviour may indicate strong adsorption of MSyr or MMC within the zeolite pores, which are subsequently converted to MGal in a later stage.

The impact of external N_2 pressure was examined by applying three different pressures: 1 bar, 10 bar, and 20 bar (Fig. S11 in the ESI†). In the context of heterogeneously catalysed ODM, external N_2 pressure is often incorporated into the

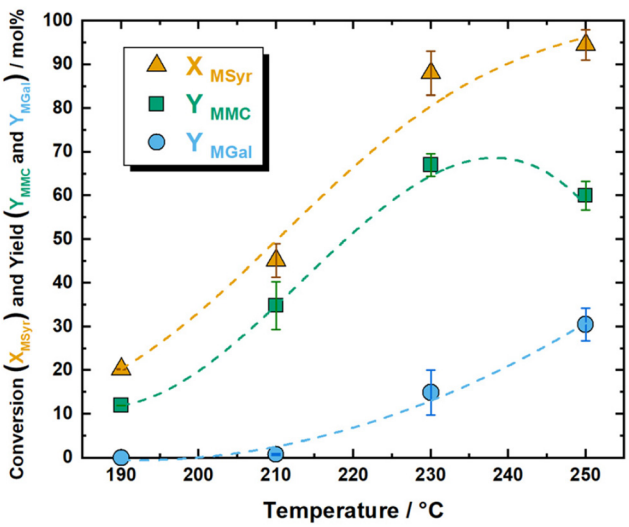

Fig. 4 Conversion of **MSyr** and yield of **MMC** and **MGal** over Beta 75 as a function of Temperature. Reaction conditions: time: 2 h, N_2 pressure 1 bar, catalyst amount: 200 mg, temperature: 190 °C, 210 °C, 230 °C, and 250 °C.

This journal is © The Royal Society of Chemistry 2025

Open Access Article. Published on 25 February 2025. Downloaded on 2/8/2026 3:04:21 PM.
This article is licensed under a Creative Commons Attribution 3.0 Unported Licence.

system. This practice appears primarily linked to maintaining consistency with homogeneous ODM, where pressure serves the specific purpose of keeping the acid in the liquid phase.[26] However, no compelling evidence has yet demonstrated the necessity of external pressure. In our experiments, we observed no significant changes in the conversion of MSyr or in the selectivity of MMC and MGal across the three pressure levels, as shown in Fig. S10 of the ESI.† Thus, we can conclude that external N_2 pressure does not influence heterogeneously catalysed ODM.

Nonetheless, a consistent mass balance gap of approximately 10 mol% was noted across all investigated conditions with Beta 75 (refer to Fig. S5 in the ESI†). To further investigate this discrepancy, TGA was performed on the spent catalyst after 2 hours of reaction under N_2 and O_2 atmospheres (Fig. S12 in the ESI†). Under N_2 flow, an initial mass loss of about 4 wt% was observed up to 600 °C, attributed to weakly bound molecules on the zeolite. When switching to O_2 at 600 °C, an additional mass loss of 2 wt% was recorded, indicating the presence of heavy (or strongly bound) organic material within the pores. This may be related to coke formation from the polycondensation of Gal moieties. However, this total mass loss of 6 wt% is insufficient to account for the 93 wt% mass balance gap, suggesting that the remaining missing material may result from the condensation of Gal moieties, which cannot be detected by GC techniques.

To further explore the chemical identity of the adsorbed species, UV-Vis adsorption spectra were recorded (Fig. S13 in the ESI†). The spectrum displayed a broad adsorption band between 250 and 450 nm, correlating with a slightly pink coloration. This spectrum was compared to that of zeolite after the isothermal adsorption of MMC, MSyr, and MGal. The Beta 75 saturated with MSyr, MMC, and MGal exhibited peaks at 276, 513, 333, and 368 nm, respectively. Notably, the adsorption peak for MMC at 513 nm corresponds to the visible light pink coloration observed in both the spent Beta 75 and during the isothermal adsorption experiment. The spent Beta 75 displayed a broad absorption band from 200 to 700 nm, which cannot be specifically attributed to a single component (Fig. S13 in ESI†). However, this band can be associated with a combination of MMC, MGal, MSyr, and the soft coke formed, as confirmed by TGA.

After 2 hours, the spent Beta 75 catalyst was selected for a reusability test and was regenerated as detailed in the Experimental section. The regenerated Beta 75 (Beta 75 R) was then tested under standard conditions, which included a reaction time of 2 hours at 210 °C and 1 bar of N_2 (Fig. S14 in ESI†). The Beta 75 R exhibited a slight decrease in both MSyr conversion (X_{MSyr}) and MMC selectivity (S_{MMC}) compared to the fresh Beta 75, with values of 45 and 27 mol% for X_{MSyr}, and 77 and 67 mol% for S_{MMC}, respectively. This reduction in activity for Beta 75 R is attributed to the zeolite's limited stability under hydrothermal conditions, which can result in amorphization, loss of crystallinity, and mesoporization of the channels. This is further supported by the observed drops in S_{BET} and V_{micro} for the spent Beta 75 compared to the fresh sample (Table S3 and Fig. S3 in ESI†). The zeolite's instability under harsh hydrothermal conditions is a well-recognized issue that poses a significant challenge to its industrial application.[46,47]

Overall, Beta zeolites demonstrated impressive selectivity across all tested conditions. When examining the selectivity in relation to conversion, the selectivity-conversion plot clearly illustrates how these zeolites enhance the selective production of MMC (Fig. S15 in ESI†). Additionally, when evaluating the MMC yield against conversion, the Beta zeolites show only slight deviations from the ideal yield-to-conversion line (Fig. 5).

To broaden the scope of the investigation, other alkyl-substituted syringyl compounds (R-Syr, where R denotes a general alkyl substituent) were tested (Fig. 6). Specifically, the non-substituted and propyl-substituted moieties, namely syringol (Syr) and 4-propyl syringol (Prop-Syr), were examined. Notably, Syr and Prop-Syr are the most common Syr compounds derived from pyrolysis and RCF wood treatment, respectively. Interestingly, altering the substituent resulted in significantly different behaviours regarding RSyr, RMC, RGal yields, and conversions. As the number of alkyl carbons increased from H- to Me- and Prop-substituted chains, the MSyr conversion exhibited a linear increase from 48 mol% to 62 mol% and then to 82 mol%. This was accompanied by a linear decrease in RMC selectivity, which dropped from 95 mol% to 82 mol% and further to 55 mol%. Along with the declines in selectivity, the RGal yield followed a similar trend, increasing from 1.3 mol% to 2.6 mol% and then to 13 mol%. This substantial difference in selectivity is combined with higher reactivity of Prop-Syr moieties, which contributes to the second ODM. Consequently, the mass balance gap was observed to increase with the size of the alkyl chain, likely due to the condensation of the more abundant Gal moieties. We hypothesize that this higher activity is due to the stronger interaction substrate-

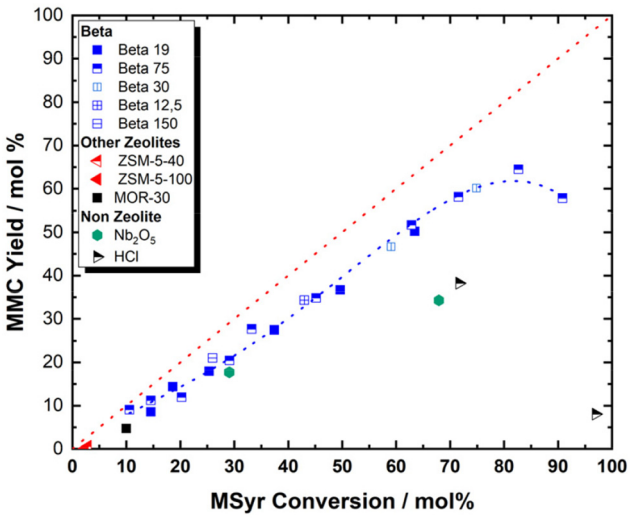

Fig. 5 MMC yield as a function of MSyr conversion. This plot summarises all the data collected in this study. The red dotted line represents the ideal yield to conversion resulting from a 100% MMC selectivity.

Open Access Article. Published on 25 February 2025. Downloaded on 2/8/2026 3:04:21 PM.
This article is licensed under a Creative Commons Attribution 3.0 Unported Licence.

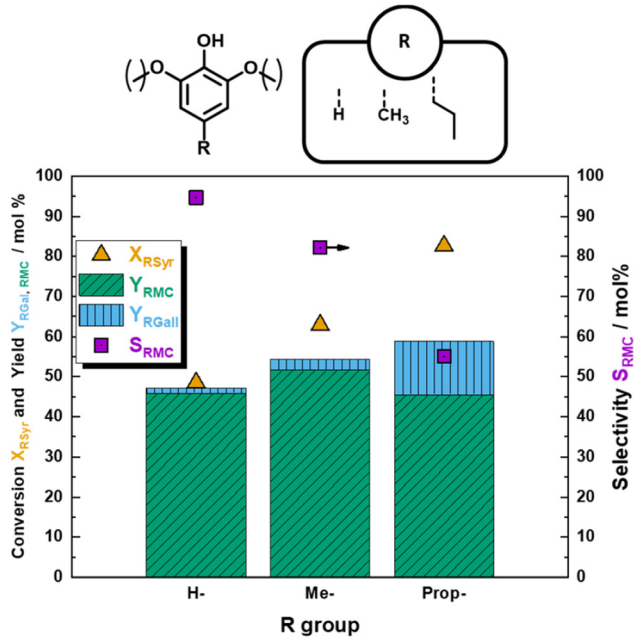

Fig. 6 Conversion of **RSyr**, selectivity of **RMC**, and Yield of **RMC** and **RGal**. Reaction conditions: time: 2 h, N_2 pressure 1 bar, catalyst amount: 200 mg, temperature: 210 °C.

zeolite interaction, which has been similarly found for different guaiacols ODM.[23]

Synthesis of MC-based epoxy thermoset

Methoxy catechol (MC), containing two vicinal phenolic hydroxyl groups, is a building block for innovative bio-derived polymers. In this study, MMC was utilized to synthesize lignin-derived epoxy thermosets *via* glycidyl functionalization. The reactivity of the two hydroxyl groups in MC is analogous to catechol, yielding the desired di-glycidylated MMC (GG-MMC) alongside the undesired methanol-dioxin or benzodioxane moiety (DX-MMC) in a 1 : 1 molar ratio, as illustrated in Scheme 4.[42] MMC was glycidylated using EC as a reactant and TEBAC as a phase-transfer catalyst (PTC), *viz.* the detailed synthesis information can be found in ESI.†

The reaction resulted in complete conversion of MMC, producing a mixture of six compounds (Fig. S16 in ESI†), characterized by GC-MS and ^{1}H-NMR and quantified *via* GC-FID (Fig. S15–19 in ESI†). The desired GG-MMC was obtained with

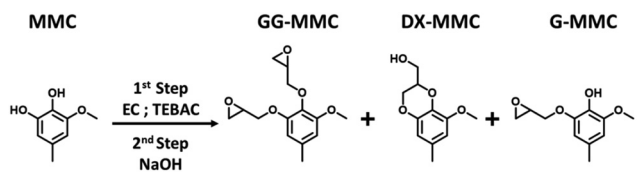

Scheme 4 Simplified MMC *O*-glycidylation toward di-glycidylated-MMC (GG-MMC), methanol-dioxin-MMC (DX-MMC), and single glycidylated-MMC (G-MMC). See Scheme S1 in ESI† for the comprehensive reaction network.

a 41 mol% yield, while DX-MMC contributed 50 mol%. Additionally, a minor product included mono-glycidylated MMC (G-MMC, 4 mol%) and mono-glycidylated hydrochlorinated MMC (GH-MMC, ≈1 mol%). No additional MMC derived compounds unit (*m*/*z* 154) were identified *via* GC-MS. However, a 4 mol% mass balance deficit, attributed to higher molecular weight products undetectable by GC or loss during work-up procedure, remains unaccounted.

The presence of six products can be attributed to the complex glycidylation mechanism, involving three competing pathways (Scheme S1, ESI†). Glycidylation occurs through either a direct nucleophilic attack on C3 of EC or *via* a two-step reaction, starting with a nucleophilic attack on C1 of EC, followed by the oxirane ring closure through dehydrochlorination. Benzodioxane species form through an intramolecular nucleophilic attack. This mechanism aligns with for similar compounds, such as 4-methyl and 4-propyl catechol, proposed by Aouf *et al.*[42] and Abu-Omar group,[48] respectively. The observed DX-MMC : GG-MMC molar ratio (50 : 41) differs from the expected 1 : 1 for catechol moieties.[42] This difference is due to the formation of unclosed GH-MMC (E–F Fig. S16B, ESI†), and G-MMC, and specific reactivity of MMC. Note that unoptimized conditions were used to produce the epoxy resins of MMC, hence, further insights into the glycidylation reaction might enhance the selectivity towards GG-MMC and allow tuning of the resin composition.

The obtained mixture was utilized without further purification to synthesize an epoxy resin thermoset, by curing with a benchmark di-amine, isophorone diamine (IPDA), at a 2 : 1 epoxy molar ratio. The epoxy concentration of the mixture was determined by NMR to be 4.19 mmol g^{-1} (Fig. S21, ESI†).

Among the components, GG-MMC actively participated in cross-linking, while G-MMC (and partially GH-MMC) serve as end units in the polymer network. In contrast, the non-glycidylated DX-MMC did not participate in the crosslinking(Fig. 7).

The cured resin, referred to as poly-IPDA-Mix, exhibited a slightly yellow polymer bar (Fig. S22, ESI†). Despite the presence of approximately 50 mol% non-crosslinked DX-MMC the curing process was completed. The thermo-mechanical properties of the produced resin were determined *via* Dynamic Mechanical Analysis (DMA), Differential Scanning Calorimetry (DSC), and Thermogravimetric Analysis (TGA) (Table S4 and Fig. S23, ESI†). The DSC of poly-IPDA-Mix resin showed a T_g of 55 °C (Fig. S23 and Table S4, ESI†), indicative of poor crosslinking degree of poly-IDPA-Mix, likely due to the plasticizing effect of non-linked DX-MMC.

The thermal stability of the poly-IPDA-Mix resin was investigated with TGA in air and N_2 (Fig. 7 and Table S4†). The thermal stability analysis showed $T_{d5\%}$ of 217 °C and T_{dmax} of 330 °C in air (211 °C and 345 °C in N_2) with a mass loss attributed to DX-MMC evaporation around 290 °C, following an approximately 25 wt% of the composite. However, due to its brittleness, the sample prevented DMA testing.

To determine (i) the impact of DX-MMC and (ii) the real properties of a highly crosslinked GG-MMC-based polymer,

 This journal is © The Royal Society of Chemistry 2025

Open Access Article. Published on 25 February 2025. Downloaded on 2/8/2026 3:04:21 PM.
This article is licensed under a Creative Commons Attribution 3.0 Unported Licence.

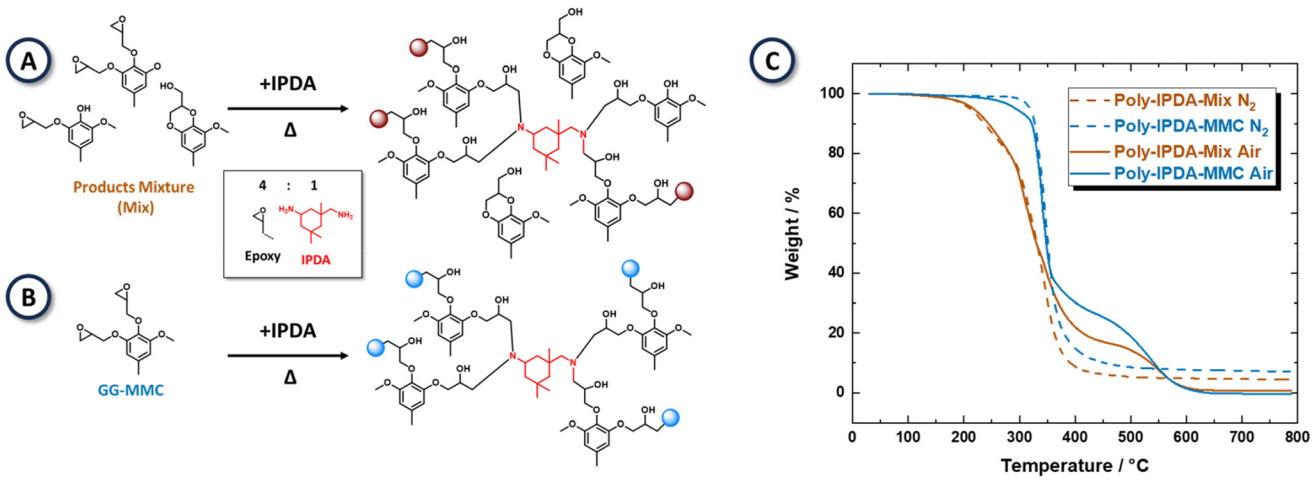

Fig. 7 Synthesis of (A) poly-IPDA-Mix and (B) poly-IPDA-MMC, see ESI† for the synthetic details. The blue and brown spheres indicate the repetition of the respective monomeric unit. (C) TGA in N_2 (dashed line) and in air (full line) of the two prepared polymers.

purified GG-MMC was isolated *via* silica column chromatography and cured in a 2 : 1 mol ratio with IPDA under identical conditions (Fig. 7). The resulting polymer bar (poly-IPDA-MMC) was transparent and characterized *via* TGA, DSC, and DMA, consisted with method described above for poly-IPDA-Mix, (Fig. 7, Table S4 and Fig. S23, 24, ESI†). The resin displayed superior thermo-mechanical properties with a T_g of 126 °C (DMA) and 119 °C (DSC) and thermal stability with a $T_{d5\%}$ of 293 °C in air and 319 °C in N_2, (Fig. 7 and Table S4†). Hence, the thermal stability of poly-IPDA-MMC is comparable to similar polymers reported in the literature, which is promising for its potential applications.[43,48]

The difference in thermo-mechanical properties between poly-IPDA-Mix and poly-IPDA-MMC is significant and is attributed to π-type interactions between the free aromatic units in the polymer. The presence of free DX-MMC (with a T_g of 55 °C) significantly lowers the T_g of the resulting resin. Interestingly, the TGA curves for both resins are similar, with T_{dmax} of 339 °C in air and around 350 °C in N_2. This indicates that the higher degradation rate involves the cured IPDA – glycidyl covalent bond. This is also confirmed by the similar behaviour of the TGA curves in N_2 above 350 °C. Overall, the presence of 50 mol% DX-MMC combined with 5 mol% of G-MMC significantly impacts the resin's mechanical properties, thermal stability and physical appearance. These findings are consistent with previous reports on lignin-derived epoxy-thermoset with different cross-linking densities.[43]

Conclusions

In this study, we present the selective single *O*-demethylation (ODM) of 4-methylsyringol (MSyr) to produce 4-methyl 6-methoxycatechol (MMC) and its subsequent application in epoxy thermoset production. This was achieved using both heterogeneous and homogeneous acidic catalysts, with Beta zeolites demonstrating optimal selectivity of 80 mol%. The 12-membered ring Beta topology played a crucial role in attaining this selectivity, outperforming other non-zeolitic catalysts, such as homogeneous acid (HCl) and heterogeneous solid acid (Nb_2O_5), as well as ZSM-5 zeolite. The density of Brønsted acid sites (BAS) in zeolites significantly influenced MSyr conversion, with optimal values at 183 μmol g^{-1}. Additionally, the reaction temperature impacted MSyr conversion and MMC selectivity, with higher temperatures favouring the formation of the Gal moiety in the second ODM. Notably, external N_2 pressure had no significant effect on the reaction products.

Further research is warranted to understand the selectivity of the first ODM, particularly focusing on zeolite size constraints and the electronic properties of the reactants and products, potentially utilizing transition state theory and theoretical simulations. Moreover, the stability of zeolites in hot water poses a challenge to industrial scalability, underscoring the need for zeolites that maintain activity under harsh hydrothermal conditions. Importantly, the use of acidic Beta zeolite in hot water for ODM of syringols (ODM) has been shown to be a more environmentally friendly process compared to traditional methods. Previous research has established that this approach significantly reduces the environmental impact associated with the treatment of syringols. In this study, we have applied this sustainable methodology to broaden the range of applications for syringols, demonstrating its potential in various innovative contexts. However, to facilitate its transition to large-scale applications, it is crucial to conduct dedicated studies focusing on cost analysis, process intensity, and techno-economic evaluations. These assessments will provide valuable insights into the feasibility and economic viability of implementing this green process on a larger scale.

The glycidylation of MMC yielded di-glycidylated (GG-MMC), benzodioxane (DX-MMC), and minor single-glycidylated products (G-MMC and GH-MMC), with respective yields of 41 mol%, 51 mol%, 5 mol%, and 1 mol%. This

Open Access Article. Published on 25 February 2025. Downloaded on 2/8/2026 3:04:21 PM. This article is licensed under a Creative Commons Attribution 3.0 Unported Licence.

finding is novel due to the limited availability of MC moieties. Although no reaction optimization was performed in this study, controlling the distribution of MMC glycidylation products remains a synthetic challenge, necessitating future studies to maximize GG-MMC yield. Two polymers were synthesized by curing with isophorone diamine (IPDA): one from the crude product mixtures (poly-IPDA-Mix) and the other from purified GG-MMC (poly-IPDA-MMC). Both polymers exhibited remarkable thermal resistance, with $T_{d5\%}$ values of 293 °C for poly-IPDA-MMC and 217 °C for poly-IPDA-Mix. Notably, the use of pure GG-MMC resulted in a transparent polymer (Fig. S22†) with an increase in T_g of 80 °C, reaching 126 °C, which could be leveraged to tailor composite materials for specific applications. It is hypothesized that the presence of 50 mol% benzodioxane significantly influences the resin's T_g and thermal stability. Future research should focus on the effects of each mixture component on the polymer properties. Furthermore, the *ortho*-methoxy group has been reported to reduce the *in vitro* estrogenic activity of phenols, suggesting that MC moieties could lower the toxicity of the polymer compared to catechol-based polymers. Therefore, future studies should evaluate the estrogenic activity of MC moieties. Herein, we have explored the application of MC for epoxy-thermoset, however multiple applications remains undiscovered, such as polymers, fragrances, antioxidant, and pharmaceuticals. Nevertheless, we have herein firstly demonstrated that MC has a yet unexploited potential to substitute fossils-derived phenols toward (partially) bio-based, and, more general, biopolymers epoxy-thermoset to investigate MC applicability for.

Overall, syringyl derivatives are the predominant components of hardwood lignin, yet their applications remain relatively unexplored. Our work emphasizes the potential of ODM in upgrading syringol moieties into a novel class of bio-based molecules, methoxy-catechols (MC), for the development of high-performance materials.

Experimental section

Materials

All the used materials were utilized as received from the supplier without any further purification, if not specified. A detailed list of the used chemicals, suppliers, and purities can be found in the ESI.†

Methods

Catalyst synthesis and characterization. All the used zeolites were calcined in static air to ensure the H-form. The layered Nb_2O_5 synthesis has been adapted from previous works.[20,44] All the details are reported in the ESI.†

MMC *O*-glycidylation. The MMC glycidylation procedure has been adapted from existing protocols in the literature.[38,42,49] The protocol employs excess of epichlorohydrin (EC) as a reactant and benzyltriethylammonium bromide (TEBAC) as a phase transfer catalyst (PTC). All the synthetic details are reported in ESI.†

Synthesis of MMC-based epoxy-thermoset. Two distinct epoxy-thermosets were synthesized, poly-IPDA-MMC and poly-IPDA-Mix, by using the GG-MMC and G-Mix resins respectively. The epoxy-resins was combined with isophorone diamine (IPDA) (molar ratio of NH_2 : epoxy 1 : 2) and cured in static air. All the synthetic details are reported in ESI.†

Data availability

The data supporting this article have been included as part of the ESI.†

Conflicts of interest

The authors declare no conflict of interest.

Acknowledgements

The authors would like to express their gratitude to Syensqo for financially supporting this study. We also extend our thanks to Walter Vermandel, Johan Maes, and Giel Dreezen from the CSCE unit of KU Leuven for their technical assistance during laboratory activities. BS acknowledges the iBOF project NextBioREF for its financial support. Additionally, we appreciate the contributions of Jing Ma and Alex Heyer from CSCE for their help with the UV-Vis analysis. Dr Deepak Raikwar from CSCE is recognized for his insightful scientific discussions. AA thanks the Erasmus+ program of the European Union for funding support. FB acknowledges the Made in Italy – Circular and Sustainable (MICS) Extended Partnership, funded by the European Union Next-Generation EU (PNRR) – (Mission 4, Component 2, Investment 1.3 – D.D. 1551.11-10-2022, PE00000004). RS acknowledges the LIBRA (Lignin-based Flame Retardants) project (G0D9923N – FWO) and the Bioeconomy initiative. LT thanks VLAIO Innovation Mandate (HBC.2023.0158) for financial support. We acknowledge the Dusselier lab (headed by prof. Michiel Dusselier) for hosting the postdoctoral grant of IK. IK acknowledges the FWO foundation for grant number 12A3M24N.

References

1 K. Collett, M. Mason, C. Williams, M. Davidson, B. O'callaghan and C. Hepburn, *Industrial need for carbon in products Final 25% Series Paper Oxford Smith School of Enterprise and the Environment*, 2021.
2 R. Meys, A. Kätelhön, M. Bachmann, B. Winter, C. Zibunas, S. Suh and A. Bardow, *Science*, 2021, **374**, 71–76.
3 W. Arts, I. Storms, J. Van Aelst, B. Lagrain, B. Verbist, J. Van Orshoven, P. J. Verkerk, V. Vermeiren, J. P. Lange, B. Muys and B. F. Sels, *Biofuels, Bioprod. Biorefin.*, 2024, **18**(2), 365–377, DOI: **10.1002/bbb.2575**.

 This journal is © The Royal Society of Chemistry 2025

Open Access Article. Published on 25 February 2025. Downloaded on 2/8/2026 3:04:21 PM. This article is licensed under a Creative Commons Attribution 3.0 Unported Licence.

4 M. Al-Naji, F. Brandi, M. Driess and F. Rosowski, *Chem. Ing. Tech.*, 2022, **94**(11), 1611–1627, DOI: **10.1002/cite.202200079**.
5 R. Rinaldi, R. Jastrzebski, M. T. Clough, J. Ralph, M. Kennema, P. C. A. Bruijnincx and B. M. Weckhuysen, *Angew. Chem., Int. Ed.*, 2016, **55**, 8164–8215, DOI: **10.1002/anie.201510351**.
6 J. Zakzeski, P. C. A. Bruijnincx, A. L. Jongerius and B. M. Weckhuysen, *Chem. Rev.*, 2010, **110**, 3552–3599, DOI: **10.1021/cr900354u**.
7 M. M. Abu-Omar, K. Barta, G. T. Beckham, J. Luterbacher, J. Ralph, R. Rinaldi, Y. Roman-Leshkov, J. Samec, B. Sels and F. Wang, *Energy Environ. Sci.*, 2021, **14**, 262–292, DOI: **10.1039/D0EE02870C**.
8 T. Renders, G. Van den Bossche, T. Vangeel, K. Van Aelst and B. Sels, *Curr. Opin. Biotechnol*, 2019, **56**, 193–201, DOI: **10.1016/j.copbio.2018.12.005**.
9 W. Arts, K. Van Aelst, E. Cooreman, J. Van Aelst, S. Van Den Bosch and B. F. Sels, *Energy Environ. Sci.*, 2023, **16**, 2518–2539, DOI: **10.1039/d3ee00965c**.
10 Y. M. Questell-Santiago, M. V. Galkin, K. Barta and J. S. Luterbacher, *Nat. Rev. Chem.*, 2020, **4**, 311–330, DOI: **10.1038/s41570-020-0187-y**.
11 Z. Sun, B. Fridrich, A. de Santi, S. Elangovan and K. Barta, *Chem. Rev.*, 2018, **118**, 614–678, DOI: **10.1021/acs.chemrev.7b00588**.
12 M. V. Galkin and J. S. M. Samec, *ChemSusChem*, 2016, **9**, 1544–1558, DOI: **10.1002/cssc.201600237**.
13 W. Schutyser, T. Renders, S. Van den Bosch, S. F. Koelewijn, G. T. Beckham and B. F. Sels, *Chem. Soc. Rev.*, 2018, **47**, 852–908, DOI: **10.1039/C7CS00566K**.
14 F. Brienza, D. Cannella, D. Montesdeoca, I. Cybulska and D. P. Debecker, *RSC Sustainability*, 2024, **2**, 37–90, DOI: **10.1039/D3SU00140G**.
15 Z. Sun, J. Cheng, D. Wang, T. Yuan, G. Song and K. Barta, *ChemSusChem*, 2020, **13**, 5199–5212.
16 B. Wang, J. Huang, H. Wu, X. Yan, Y. Liao and H. Li, Synergy of heterogeneous Co/Ni dual atoms enabling selective C–O bond scission of lignin coupling with in-situ N-functionalization, *J. Energy Chem.*, 2024, **92**, 16–25.
17 X. Wu, E. Smet, F. Brandi, D. Raikwar, Z. Zhang, B. U. W. Maes and B. F. Sels, *Angew. Chem., Int. Ed.*, 2024, **136**(10), e202317257, DOI: **10.1002/anie.202317257**.
18 F. M. Harth, B. Hočevar, T. R. Kozmelj, E. Jasiukaitytė-Grojzdek, J. Blüm, M. Fiedel, B. Likozar and M. Grilc, *Green Chem.*, 2023, **25**, 10117–10143, DOI: **10.1039/D3GC02867D**.
19 J. Bomon, M. Bal, T. K. Achar, S. Sergeyev, X. Wu, B. Wambacq, F. Lemière, B. F. Sels and B. U. W. Maes, *Green Chem.*, 2021, **23**, 1995–2009, DOI: **10.1039/D0GC04268D**.
20 X. Wu, Y. Liao, J. Bomon, G. Tian, S.-T. Bai, K. Van Aelst, Q. Zhang, W. Vermandel, B. Wambacq, B. U. W. Maes, J. Yu and B. F. Sels, *ChemSusChem*, 2022, **15**(7), e202102248, DOI: **10.1002/cssc.202102248**.
21 B. Liu, M. Sanchez, J. Truong, P. C. Ford and M. M. Abu-Omar, *Green Chem.*, 2022, **24**, 4958–4968, DOI: **10.1039/d2gc01278b**.
22 M. Bocus, E. Van Den Broeck, X. Wu, M. Bal, J. Bomon, L. Vanduyfhuys, B. F. Sels, B. U. W. Maes and V. Van Speybroeck, *Nat. Catal.*, 2025, **8**, 33–45, DOI: **10.1038/s41929-024-01282-6**.
23 X. Wu, M. Bal, Q. Zhang, S. T. Bai, I. Scodeller, W. Vermandel, J. Yu, B. U. W. Maes and B. F. Sels, *J. Am. Chem. Soc.*, 2025, **147**(6), 4915–4929, DOI: **10.1021/jacs.4c13729**.
24 F. Brandi, B. Pandalone and M. Al-Naji, *RSC Sustainability*, 2023, **1**, 459–469, DOI: **10.1039/D2SU00076H**.
25 Z. Li, E. Sutandar, T. Goihl, X. Zhang and X. Pan, *Green Chem.*, 2020, **22**, 7989–8001, DOI: **10.1039/D0GC02581J**.
26 B. Maes, J. Bomon, S. Sergueev and E. Blondiaux, Methods for the deacyation and/or dealkylation of compounds, WO2019025535A1, World Intellectual Property Organization, 2018.
27 Y. Wang, M. Chen, Y. Yang, J. Ralph and X. Pan, *RSC Adv.*, 2023, **13**, 5925–5932, DOI: **10.1039/D3RA00245D**.
28 B. Maes, J. Bomon, S. Sergueev and E. Blondiaux, Methods for the deacyation and/or dealkylation of compounds, WO2019025535A1, World Intellectual Property Organization, 2018.
29 J. Zhang, Q. Qian, Y. Wang, B. Baffour, A. Bediako, J. Yan and B. Han, *Chem. Sci.*, 2019, **10**, 10640–10646, DOI: **10.1039/C9SC03386F**.
30 B. Maes, J. Bomon, S. Sergueev and E. Blondiaux, Methods for the deacyation and/or dealkylation of compounds, WO2019025535A1, World Intellectual Property Organization, 2018.
31 A. L. Jongerius, R. Jastrzebski, P. C. A. Bruijnincx and B. M. Weckhuysen, *J. Catal.*, 2021, **285**, 315–323, DOI: **10.1016/j.jcat.2011.10.006**.
32 V. N. Bui, D. Laurenti, P. Afanasiev and C. Geantet, *Appl. Catal., B*, 2011, **101**(3–4), 239–245, DOI: **10.1016/j.apcatb.2010.10.025**.
33 S. Zhao and M. M. Abu-Omar, *ACS Sustainable Chem. Eng.*, 2017, **5**(6), 5059–5066, DOI: **10.1021/acssuschemeng.7b00440**.
34 J. Zhang, Y. S. Cheah, S. Santhanakrishnan, K. G. Neoh and C. L. L. Chai, *Polymer*, 2017, **116**, 5–15, DOI: **10.1016/j.polymer.2017.03.061**.
35 B. F. Sels, L. Trullemans, S. Koelewijn, I. Scodeller, T. Hendrickx and P. Van Puyvelde, *Polym. Chem.*, 2021, **12**, 5870–5901, DOI: **10.1039/D1PY00909E**.
36 S. Wang, A. W. Bassett, G. V. Wieber, J. F. Stanzione and T. H. Epps, *ACS Macro Lett.*, 2017, **6**, 802–807, DOI: **10.1021/acsmacrolett.7b00381**.
37 H. T. H. Nguyen, P. Qi, M. Rostagno, A. Feteha and S. A. Miller, *J. Mater. Chem. A*, 2018, **6**, 9298–9331, DOI: **10.1039/C8TA00377G**.
38 L. Trullemans, S.-F. Koelewijn, I. Boonen, E. Cooreman, T. Hendrickx, G. Preegel, J. Van Aelst, H. Witters, M. Elskens, P. Van Puyvelde, M. Dusselier and B. F. Sels, *Nat. Sustain.*, 2023, **6**, 1693–1704, DOI: **10.1038/s41893-023-01201-w**.
39 S.-F. Koelewijn, D. Ruijten, L. Trullemans, T. Renders, P. Van Puyvelde, H. Witters and B. F. Sels, *Green Chem.*, 2019, **21**, 6622–6633, DOI: **10.1039/C9GC02619C**.

Open Access Article. Published on 25 February 2025. Downloaded on 2/8/2026 3:04:21 PM.
This article is licensed under a Creative Commons Attribution 3.0 Unported Licence.

40 M. Asmadi, H. Kawamoto and S. Saka, *J. Anal. Appl. Pyrolysis*, 2011, **92**, 88–98, DOI: **10.1016/j.jaap.2011.04.011**.
41 B. Liu, M. Sanchez, J. Truong, P. C. Ford and M. M. Abu-Omar, *Green Chem.*, 2022, **24**, 4958–4968, DOI: **10.1039/d2gc01278b**.
42 C. Aouf, C. Le Guernevé, S. Caillol and H. Fulcrand, *Tetrahedron*, 2013, **69**, 1345–1353, DOI: **10.1016/j.tet.2012.11.079**.
43 S. Zhao and M. M. Abu-Omar, *ACS Sustainable Chem. Eng.*, 2016, **4**(11), 6082–6089, DOI: **10.1021/acssuschemeng.6b01446**.
44 T. Murayama, J. Chen, J. Hirata, K. Matsumoto and W. Ueda, *Catal. Sci. Technol.*, 2014, **4**, 4250, DOI: **10.1039/C4CY00713A**.
45 I. Khalil, K. Thomas, H. Jabraoui, P. Bazin and F. Maugé, *J. Hazard. Mater.*, 2020, **384**, 121397, DOI: **10.1016/j.jhazmat.2019.121397**.
46 F. Brandi, I. Khalil, M. Antonietti and M. Al-Naji, *ACS Sustainable Chem. Eng.*, 2021, **9**, 927–935, DOI: **10.1021/acssuschemeng.0c08167**.
47 L. Zhang, K. Chen, B. Chen, J. L. White and D. E. Resasco, *J. Am. Chem. Soc.*, 2015, **137**, 11810–11819, DOI: **10.1021/jacs.5b07398**.
48 S. Zhao and M. M. Abu-Omar, *Macromolecules*, 2019, **52**(10), 3646–3654, DOI: **10.1021/acs.macromol.9b00334**.
49 B. F. Sels, L. Trullemans, S. Koelewijn, I. Scodeller, T. Hendrickx and P. Van Puyvelde, *Polym. Chem.*, 2021, **12**, 5870–5901, DOI: **10.1039/D1PY00909E**.

This journal is © The Royal Society of Chemistry 2025